ANNALI DI BOTANICA
Ann. Bot. (Roma), 2016, 6: 93–99
Journal homepage: http://annalidibotanica.uniroma1.it

DEVELOPMENT OF FLUORESCENCE INDICES TO MINIMISE THE EFFECTS OF CANOPY STRUCTURAL PARAMETERS

COLOMBO R.[1*], MERONI M.[2], ROSSINI M.[1]

[1]*Remote Sensing of Environmental Dynamics Lab., DISAT, Università di Milano-Bicocca, P.zza della Scienza 1, 20126 Milano, Italy*
[2]*European Commission, Joint Research Centre, Institute for Environment and Sustainability, Via E. Fermi 2749, I-21027 Ispra (VA), Italy*
[*]*Corresponding Author: Telephone: +39 02 64482819; email: roberto.colombo@unimib.it*

(RECEIVED 05 APRIL 2016; RECEIVED IN REVISED FORM 19 APRIL 2016; ACCEPTED 20 APRIL 2016)

ABSTRACT – Remote Sensing of Sun-Induced Chlorophyll Fluorescence is a research field of growing interest with the potential to provide an improved tool for monitoring plant status and photosynthetic function. The new satellite mission of the European Space Agency (the FLuorescence EXplorer, FLEX) will provide the possibility to estimate canopy fluorescence from space at global level. However, remote sensing techniques allow measurement of the emitted fluorescence flux but do not provide a direct assessment of the fluorescence yield, which is the key variable linked to the physiological status of the plant.
In this study, we investigate the impact of canopy structure on chlorophyll fluorescence by analysing the fluorescence emission in a thinning experiment in a corn field. It is shown that fluorescence and apparent fluorescence yield are well related with leaf area index and vegetation fractional cover, but when fluorescence is divided for a spectral vegetation index (considered as a proxy of structural parameters) the correlation is lost. This means that fluorescence indexes should be considered to take into account spatial and temporal variability of biophysical parameters for satellite studies and promising for plant status applications.

KEYWORDS: SUN-INDUCED CHLOROPHYLL FLUORESCENCE, BIOPHYSICAL PARAMETERS, ESA-FLEX MISSION

INTRODUCTION

Sun-Induced Chlorophyll Fluorescence is an electromagnetic signal emitted in the red and near-infrared regions by the vegetation chlorophyll in response to the absorption of photosynthetically active radiation. This low signal (1–5% of the reflected radiation in the near- infrared) is directly emitted by the photosynthetic apparatus. In the last decades, several researches have demonstrated the potential use of fluorescence to monitor photosynthesis and the functional status of vegetation (Corp et al., 2003; Maier et al., 2003; Meroni & Colombo, 2006, Buschmann, 2007; Campbell et al., 2007; 2008; Damm et al., 2010; Zarco-Tejada et al., 2012, 2013; Panigada et al., 2014). In recent years, the increasing number of scientific studies attests the growing interest of the remote sensing community (Meroni et al., 2009, Frankenberg et al., 2014, Hand, 2014) at different scales of investigations. Recently, Member States of the European Space Agency (ESA) have selected FLEX (FLuorescence EXplorer, ESA, 2015) as the eighth Earth Explorer mission, upon recommendation from the Earth Science Advisory Committee. The FLEX mission aims to provide global maps of vegetation fluorescence at 300 m spatial resolution, which can be used to infer photosynthetic activity of natural and managed ecosystems. This information is critical to gain understanding of carbon exchange between the biosphere and the atmosphere and to improve predictions on how vegetated ecosystems contribute to the carbon and water cycles.

doi: 10.4462/annbotrm-13273

However measuring plant fluorescence is challenging and algorithm development, as well as dedicated experiments at field and at airborne level, are mandatory for demonstrating the feasibility of measuring this emitted signal using remote sensing instruments (e.g. Rascher et al., 2009; 2015).
To tackle this need, different field and airborne activities for the measurement of fluorescence are currently conducted under the FLEX umbrella (e.g. Colombo et al., 2014; Rossini et al., 2015). In addition, numerous modelling studies aiming at the development of innovative retrieval algorithms for space applications, are also under investigation (e.g. Cogliati et al., 2015).
There are some fundamental challenges in plant status assessment using solar induced fluorescence. Besides plant physiological status, other factors that alter the fluorescence signal are bidirectional effects, background response, atmosphere and variability of structural parameters. In addition, fluorescence responds to changes in the incoming radiation and changes in space due to the variability of canopy parameters. In this context, there is a need to have fluorescence quantities independent from leaf amount and canopy parameters (such as leaf angle distribution or clumping). It is therefore extremely important to develop algorithms for minimizing the effects of green biomass/chlorophyll on the recorded signal. In fact, the intensity of the fluorescence signal at canopy level depends both on the efficiency of the photosynthetic apparatus and from the chlorophyll content. Therefore, in order to correctly interpret the fluorescence signal as an indicator of photosynthetic efficiency a normalization of the signal for the chlorophyll content of the investigated target is needed. Canopy with different photosynthetic efficiency and chlorophyll content can in fact lead to the same fluorescence signal.
The maximum rate of carboxylation is a key control parameter of photosynthetic capacity. However, according to the recent Global Sensitivity Analysis of the Soil Canopy Observation, Photochemistry and Energy Fluxes (SCOPE) model (Verrelst et al., 2015), it drives only a relatively small portion of the fluorescence signal. Broadband incoming shortwave radiation, leaf chlorophyll content, and leaf area index (LAI) are major drivers of fluorescence emission intensity. Therefore, if variations in the spatial and temporal domains of these drivers are not properly accounted for, remotely sensed fluorescence flux could be not properly interpreted.
To investigate how fluorescence is sensitive to biomass, we conducted a progressive cutting experiment in a corn field in the framework of the ESA-CESFLES2 campaigns in Marmande (France). Spectral measurements were performed on an undisturbed corn canopy and at the same time on corn plot subjected to thinning (i.e., artificial LAI reduction) with the objective of developing and testing fluorescence indices independent of canopy structural parameters.

Materials and Methods

Spectral data acquisition and processing

Fluorescence measurements were obtained by using a portable spectrometer OceanOptics HR4000 operating in the range 707-805 nm, Full Width at Half Maximum (FWHM) 0.1 nm (hereafter named CF, Chlorophyll Fluorescence). This spectrometer was employed for the estimation of the chlorophyll fluorescence in the oxygen A band, while a second spectrometer operating in the range of 198-1120 nm, FWHM 2.8 nm (hereafter named FS, Full Spectrum), was instead used for the computation of the Photochemical Reflectance Index and other optical vegetation indexes.
Prior to the field campaign both spectrometers were calibrated with known standards (wavelength calibration and radiance calibration). A calibrated white reference panel (50x50 cm 90% reflectance, Optopolymer GmbH, Germany) was employed to estimate the incident irradiance.
Measurements were acquired on the 23rd of April 2007 on a corn field, using bare fibers and viewing the target from nadir. We employed the field spectroscopy technique referred to as 'single beam' (Milton and Rolling 2006): target measurements are 'sandwiched' between two reflectance standard panel measurements made a few seconds apart. The radiance of the reference panel at the time of the target measurement is estimated by linear interpolation. This technique is based on the assumption that incident irradiance varies linearly between the two reference panel measurements. For every spectral acquisition, 4 and 15 scans (for the CF and FS spectrometers, respectively) were averaged and stored as a single file. Additionally, a dark current measurement was collected for every subset of acquisitions (usually 4). Spectrometers were housed in a Peltier thermally insulated box (model NT-16, Magapor, Zaragoza, Spain) keeping the internal temperature at 25°C in order to reduce dark current drift.
Spectral data were acquired and processed with dedicated software developed by the remote sensing laboratory of the University of Milano-Bicocca: 3S for field acquisition and OO_IDL for processing (Meroni & Colombo 2009). Processing of raw data included: i) correction for Charge-Coupled Device (CCD) detector non linearity, ii) correction for dark current and dark current drift, iii) wavelength calibration and linear resampling, iv) radiance calibration and v) incident radiance computation by linear interpolation of two white reference measurements and correction for the known white reflectance.
The spectrometric system was installed on top of a two floors

scaffolding tower targeting the corn field from a distance of 2.2m. A circular area of the canopy with 49 cm radius was observed by the spectrometers. The rotation of a mast mounted horizontally on a tripod (placed on the top floor) permitted to observe, with spectrometer bare fibers, either the white reference panel or the corn plant samples (Figure 1).

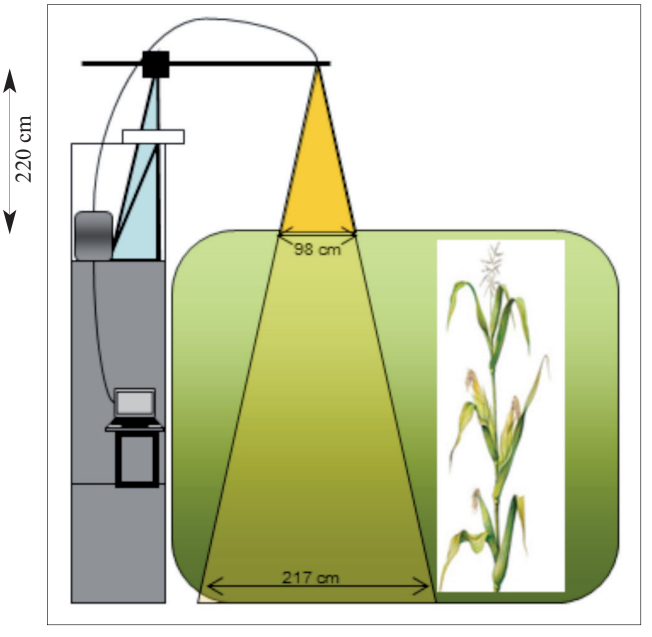

Figure 1. Sampling set-up at the corn field.

After the basic processing, the radiance upwelling from the target, and the target HCRF (Hemispherical Conical Reflectance Factor), was obtained.

Computation of fluorescence and fluorescence yields

Fluorescence (Fs) was computed from the CF spectrometer data considering a linear variation of reflectance and fluorescence according to Meroni & Colombo (2006). Lin@750 nm is the incident radiance measured in the range 747.22-758.76 nm. NF is the Normalized Fluorescence, i.e. the ratio between estimated fluorescence and the radiation incident in a nearby restricted spectral range not including the absorption line (i.e., in the *continuum,* 747.22-758.76 nm). Therefore, NF= Fs/Lin @750 nm.

LAI reduction experiment

Two non-overlapping areas were observed from nadir thanks to the rotating must positioned at the scaffolding tower top floor. One area was undisturbed while the other was progressively thinned during a two and a half hour experiment. Thinning started at 10:20 UTC with the removal of 2 'columns' of plants and continued with successive 'column' removal (3 plants at a time) until thinning the last plants at 12:35 UTC when the last two 'columns' were removed leaving bare soil in the area observed by the spectrometers..

Hemispherical photographs were acquired with a NIKON 8400 Coolpix digital camera equipped with a FC-E9 8mm fisheye lens converter in order to estimate LAI and vegetation Fractional Cover (Fc). Each LAI and Fc were obtained along a transect, diagonally crossing the plantation rows. Plantation rows were spaced of about 80 cm while along the row, the plants spacing was about 20 cm. The transect length (1.4 m), and the spatial interval between ground samples (0.35 m) were fixed, and a single LAI and Fc value was obtained by averaging four samples (four images) collected along the transect. The computation of the effective LAI and Fc was conducted by using the Can_Eye software (Martinez et al., 2004).

Results

Spectral data

The difference between the data collected with the two spectrometers is illustrated in Figure 2.

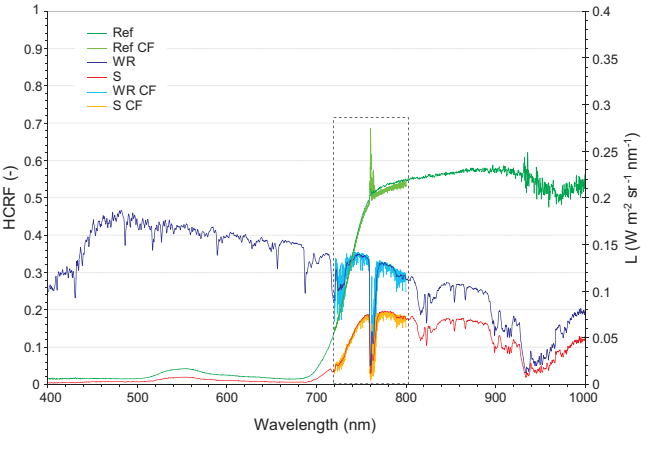

Figure 2. Spectral data gathered with a single data acquisition from the two spectrometers. FS spectrometer covers without noise the range 400-1000 nm while the CF spectrometer covers the range 720-805 nm. Incident radiance is in blue (light blue) for FS (CF) spectrometers. The radiance upwelling from the canopy is red (yellow) for the FS (CF). The corresponding reflectance is in green (light green) for the FS (CF) spectrometers. It is evident the fluorescence peak at 760 nm, superimposed on the reflectance curve.

Canopy fluorescence at different thinning

The experiment was conducted around solar noon in order to have only a moderate variation in the incident solar irradiance and fluorescence (under such conditions, leaf physiology should not change during the experiment, although this may be not completely true). An example of the digital images collected at different thinning is shown in Figure 3. G1 represents the undisturbed plot (control), while the Z to O pictures depict the progressive thinning applied (Z being the initial conditions and O the final stage when almost only bare soil was seen by the spectrometer). That is, we used this scheme to acquire data in a progressive thinning experiment in which we removed 6 plants at each time. Lower graphics of Figure 3 show the decrease of LAI and Fc during the experiment. Although LAI and Fc may not be exactly computed in correspondence to the area observed by the spectroradiometer, the decreasing trend operated by the subsequent cutting is clear (Figure 3).

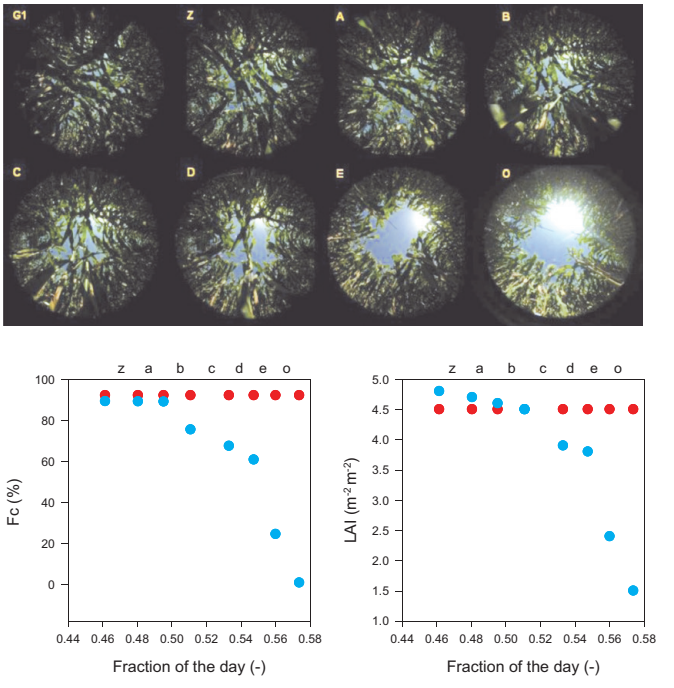

Figure 3. Hemispherical photos collected upward at each thinning step and its effect on Fc and LAI. Red and blue dots refer to control (undisturbed) and treatment (progressively thinned) areas, respectively. Graphics use "dayfract" which is the fraction of the day in local solar time (e.g. local solar noon, 12:00, is dayfract 0.5 and UTC 11:00).

The external cuts *z*, *a* and *b* are well seen by reflectance indices variation, as shown in the vegetation indices (data not shown). The cutting of the internal six plants c and d provokes a decrease in LAI and causes a decrease in vegetation indices (namely Normalised Difference Vegetation Index -NDVI and Simple Ratio -SR, data not shown). After the removal of the central plants in e the value of LAI dramatically decreases and the spectral measurements can be regarded as that of bare soil. Also the spectral measurements after the removal of the most external plants refer to bare soil, as demonstrated by the same values of optical indices. As expected the observed reflectance was affected by thinning (Figures 4).

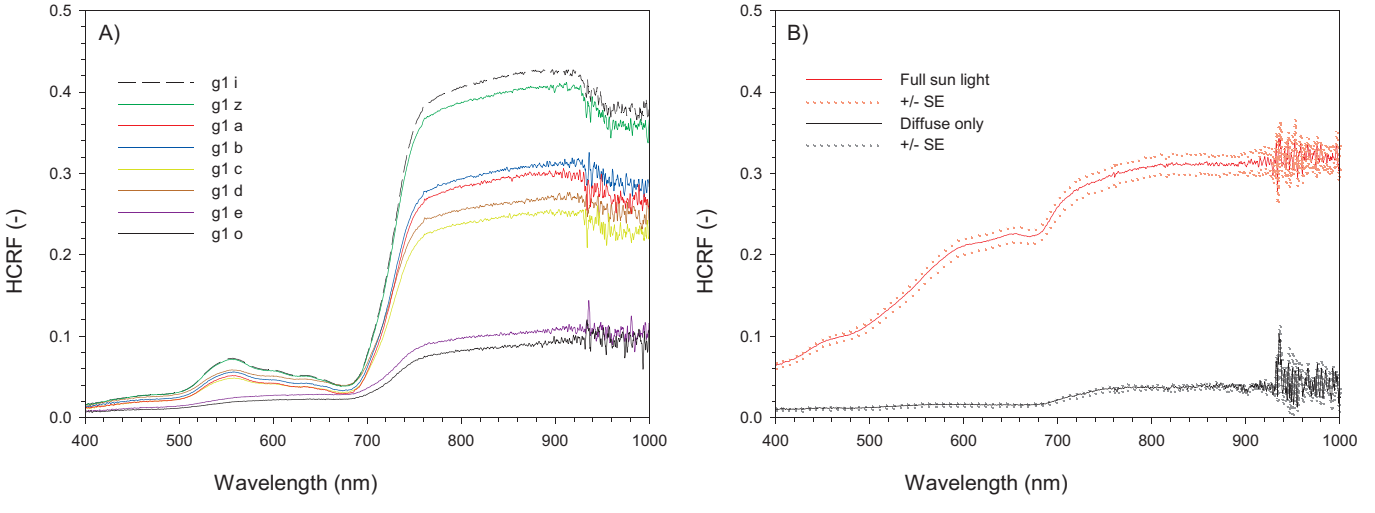

Figure 4. Average HRCF (4 consecutive measurements) of: A) manipulation area after progressive thinning and, B) bare soil (when illuminated by full sun light, red curve, and when illuminated only by the diffuse solar light, black curve). SE is the standard error of the measurements.

The black continuous curve in figure 4 (A) refers to the last thinning step (o) when the soil background was completely exposed. The comparison with this curve with that of the bare soil (a clod removed from the ground was measured in full sunlight) in different illumination condition (full light and shadow) confirms the field observation that the area observed by the sensor was composed by a mixture of sunlit and shaded soil. This effect is due to the fact that thinning was limited to few square meters around the sampling area because of logistic reasons. Therefore, after the complete removal of the plants, the area observed by the spectrometer was represented by soil surrounded by tall corn plant 'walls'. Besides cast shadows, another 3D effect arising in this conditions is that the lateral flux of photons may not be negligible (i.e. photons scattered by the plants surrounding the clearing into it and then scattered again by the soil into to the observation direction).

The treatment fluorescence is decreased of about 30 % at dayfract=0.52 as a result of thinning steps *z*, *a*, *b* (Figure 5). The steps *c* and *d* slightly affect fluorescence, while step *e*, which refers to the removal of the plant in the centre of the field of view, strongly affect the fluorescence (about 70% decrease).

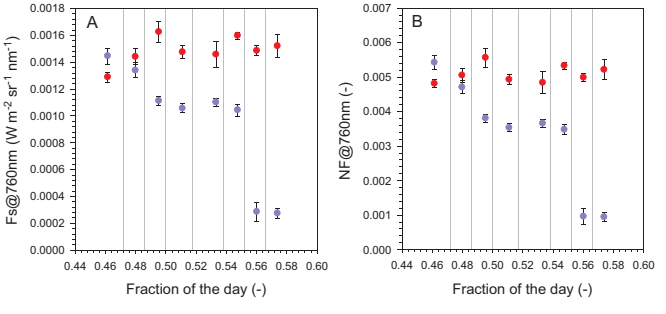

Figure 5. A) Fluorescence at oxygen A band (760 nm) and B) NF@760nm, Normalized Fluorescence at 760 nm (i.e. Fs/Lin). Red and violet dots refer to control (undisturbed) and treatment (progressively thinned) areas, respectively. Vertical lines above the X axis in A) refer to thinning steps. Spectral measurements in the graphs are the average of data acquired in each thinning time interval (from 4 to 8 consecutive measurements). Error bars refer to ±1SE.

Fluorescence and normalized fluorescence are significantly related with LAI and Fc, as observed in other studies (e.g. Olioso et al., 1992) (Figure 6), although with poorer correlation coefficients than those found using optical indices (data not shown). Under the assumption that the physiological status of the standing should not change during the experiment (i.e., should be insensitive to standing LAI), the observed dependency of fluorescence to LAI indicates the need to separate the effects of LAI in the fluorescence retrieval at canopy level. In other words, if we are interested in describing the plant physiological status (for example for stress detection or for estimating the light use efficiency) it would be desirable to have a fluorescence index independent by LAI or other structural parameters.

Here we propose to obtain such an index by dividing the NF by the LAI to get a NF per unit LAI area. Figure 6 shows that using the normalized fluorescence index, obtained dividing NF by the Simple Ratio vegetation index (SR assumed to be a good proxy of LAI or the fraction of the absorbed photosynthetically active radiation, fAPAR), the correlation with LAI is lost. It should be noted that this simple fluorescence index, having at denominator the incident radiation and fAPAR) is also a proxy of the actual fluorescence yield, the fluorescence emission per unit of absorbed PAR.

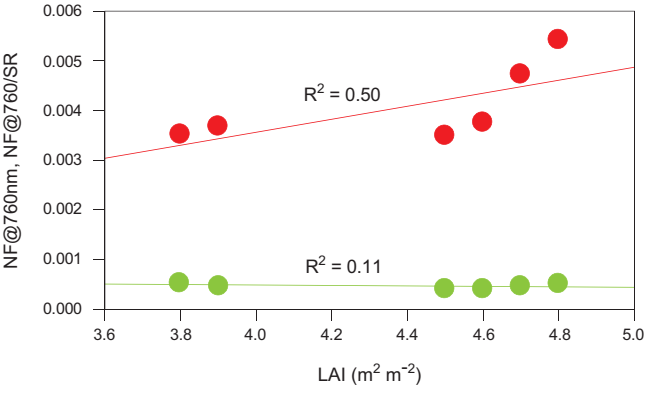

Figure 6. Red and green dots represent NF@760 and NF@760/SR, respectively.

With this exercise we empirically showed that it is possible to construct a fluorescence index largely insensitive to LAI variations but with the data at hand we cannot demonstrate that the proposed index is indeed sensitive to leaf physiological status. Future studies should be aimed to evaluate the proposed index or other forms of the actual fluorescence yield (i.e. fluorescence divided by APAR) as indicators of the plant status.

Conclusions

New instruments, new data and knowledge and a new generation of retrieval schemes have been recently developed in the context of the FLEX mission. Results obtained from these studies are promising although challenges and uncertainties still remain, but they direct towards demonstrating the capability of this mission in observing the

environment with new perspectives.
Canopy chlorophyll fluorescence depends on the variation of individual leaf response inside the canopy, the attenuation of incident exciting radiation, and the scattering of emitted radiation toward the sensor. Several studies suggest that canopy structure affects canopy fluorescence. These structural effects are quite important, they interact with the other fluorescence variation factors, and they must be taken into consideration to interpret measurements, especially for plant status analysis. In this study we designed a field experiment to evaluate the impact of canopy structure on solar induced fluorescence.
A simple fluorescence index is presented which takes into account the structural variations of the canopy. Analysis shows that canopy fluorescence is strongly affected by leaf area index and vegetation fractional cover parameters. However, the use of the fluorescence ratio based on the knowledge of the simple ratio vegetation index can limit these effects.

REFERENCES

Buschmann C., 2007. Variability and application of the chlorophyll fluorescence emission ratio red/far-red of leaves. Photosynthesis Research 92, 261-71.

Campbell P.K.E., Middleton E.M., Corp L.A., Kim M.S., 2008. Contribution of chlorophyll fluorescence to the apparent vegetation reflectance. Science of the Total Environment 404, 433-9.

Campbel, P.K.E., Middleton E.M., McMurtrey J.E., Corp L.A., Chappelle E.W., 2007. Assessment of vegetation stress using reflectance or fluorescence measurements. Journal of Environmental Quality 36, 832-45.

Cogliati S., Verhoef W., Kraft S., Sabater N., Alonso L., Vicent J., Moreno J. Drusch M., Colombo R., 2015. Retrieval of sun-induced fluorescence using advanced spectral fitting methods. Remote Sensing of Environment 169, 344-357.

Colombo R., Alonso L., Celesti M., Cogliati S., Damm A., Drusch M., Guanter L., Julitta T., Kokkalis P., Moreno J., Panigada C., Pinto F., Rascher U., Rossini M., Schickling A., Schüttemeyer D., Verhoef W., Zemek F., 2014. Remote sensing of sun-induced chlorophyll fluorescence at different scales. 6th Workshop on Hyperspectral Image and Signal Processing (WHISPERS): Evolution in Remote Sensing, Lausanne, Switzerland, 24-27 June 2014, 4 pp.

Corp L.A., McMurtrey J.E., Middleton E.M., Mulchi C.L., Chappelle E.W., Daughtry C.S., 2003. Fluorescence sensing systems: In vivo detection of biophysical variations in field corn due to nitrogen supply. Remote Sensing of Environment 86, 470-479.

Damm A., Elbers J., Erler A., Gioli B., Hamdi K., Hutjes R., Kosvancova M., Meroni M., Miglietta F., Moersch A., Moreno J., Schickling A., Sonnenschein R., Udelhoven T., Van Der Linden S., Hostert P., Rascher U., 2010. Remote sensing of sun-induced fluorescence to improve modeling of diurnal courses of gross primary production (GPP). Global Change Biology 16, 171-186.

ESA, 2015. Report for Mission Selection: FLEX, ESA SP-1330/2 (2 volume series), European Space Agency, Noordwijk, The Netherlands.

Frankenberg C., O'Dell C., Berry J., Guanter L., Joiner J., Köhler P., Pollock R., Taylor T.E., 2014. Prospects for chlorophyll fluorescence remote sensing from the Orbiting Carbon Observatory-2. Remote Sensing of the Environment 147, 1-12.

Hand E., 2014. Carbon-mapping satellite will monitor plants' faint glow. Science 344, 1211-1212.

Maier S.W., Günther K,P., Stellmes M., 2003. Sun-induced fluorescence: A new tool for precision farming. In: M. McDonald, J. Schepers, L. Tartly, T. VanToai and D. Major (Eds) Digital Imaging and Spectral Techniques: Applications to Precision Agriculture and Crop Physiology. ASA Special Publication Vol 66, p. 209-222.

Martínez B., Baret F., Camacho-de Coca F., García-Haro F.J., Verger A., Meliá J., 2004. Validation of MSG vegetation products Part I. Field retrieval of LAI and FVC from hemispherical photographs. In: M. Owe G. D'Urso, B.T. Gouweleeuw and A.M. Jochum (Eds) Remote Sensing for Agriculture, Ecosystem and Hydrology; SPIE, Bellingham, WA, 2004; Vol. 5568, pp. 57-68. Sensing for Agriculture, Ecosystems, and Hydrology VI, 57.

Meroni M., Colombo R., 2006. Leaf level detection of solar induced chlorophyll fluorescence by means of a subnanometer resolution spectroradiometer, Remote Sensing of Environment 103(4), 438-448.

Meroni M., Rossini M., Guanter L., Alonso L., Rascher U., Colombo R., Moreno J., 2009. Remote sensing of solar-induced chlorophyll fluorescence: Review of methods and applications. Remote Sensing of Environment 113, 2037-2051.

Milton E.J., Rollin E.M., 2006. Estimating the irradiance spectrum from measurements in a limited number of spectral bands. Remote Sensing of Environment 100, 348-355.

Olioso A., Methy M., Lacaze B., 1992. Simulation of Canopy

Fluorescence as a Function of Canopy Structure and Leaf Fluorescence. Remote Sensing of Environment 41, 239-247.

Panigada C., Rossini M., Meroni M., Cilia C., Busetto L., Amaducci S., Boschetti, M., Cogliati S., Picchi V., Pinto F., Marchesi A., Colombo R., 2014. Fluorescence, PRI and canopy temperature for water stress detection in cereal crops. International Journal of Applied Earth Observation and Geoinformation 30, 167-178.

Rascher U., Alonso L., Burkart A., Cilia C., Cogliati S., Colombo R., Damm A., Drusch M., Guanter L., Hanus J., Hyvärinen T., Julitta T., Jussila J., Kataja K., Kokkalis P., Kraft S., Kraska T., Matveeva M., Moreno J., Muller O., Panigada C., Pikl M., Pinto F., Prey L., Pude R., Rossini M., Schickling A., Schurr U., Schüttemeyer D., Verrelst J., Zemek F., 2015. Sun-induced fluorescence – a new probe of photosynthesis: First maps from the imaging spectrometer HyPlant. Global Change Biology 21, 4673-4684.

Rascher U., Agati G., Alonso L., Cecchi G., Champagne S., Colombo R., Damm A., Daumard F., de Miguel E., Fernandez G., Franch B., Franke J., Gerbig C., Gioli B., Gomez J.A., Goulas Y., Guanter L., Gutierrez-de-la-Camara O., Hamdi K., Hostert P. Jimenez M., Kosvancova M., Lognoli D., Meroni M., Miglietta F., Moersch A., Moreno J., Moya I., Neininger B., Okujeni A., Ounis A., Palombi L., Raimondi V., Schickling A., Sobrino J.A., Stellmes M., Toci G., Toscano P., Udelhoven T. , Van der Linden S., Zaldei A., 2009. CEFLES2: the remote sensing component to quantify photosynthetic efficiency from the leaf to the region by measuring sun-induced fluorescence in the oxygen absorption bands. Biogeosciences, 6, 1181-1198.

Rossini M., Nedbal L., Guanter L., Ač A., Alonso L., Burkart A., Cogliati S., Colombo R., Damm A., Drusch M., Hanus J., Janoutova R., Julitta T., Kokkalis P., Moreno J., Novotny J., Panigada C., Pinto F., Schickling A., Schüttemeyer D., Zemek F., Rascher U., 2015. Red and far-red sun-induced chlorophyll fluorescence as a measure of plant photosynthesis. Geophysical Research Letters 42, 1632-1639.

Verrelst J., Rivera J.P., van der Tol C., Magnani F., Mohammed G., Moreno J., 2015. Global sensitivity analysis of the SCOPE model: What drives simulated canopy-leaving sun-induced fluorescence? Remote Sensing of Environment 166, 8-21.

Zarco-Tejada P.J., González-Dugo V., Berni J.A.J., 2012. Fluorescence, temperature and narrow-band indices acquired from a UAV platform for water stress detection using a micro-hyperspectral imager and a thermal camera. Remote Sensing of Environment 117, 322-337.

Zarco-Tejada P.J., Morales A., Testi L., Villalobos F.J., 2013. Spatio-temporal patterns of chlorophyll fluorescence and physiological and structural indices acquired from hyperspectral imagery as compared with carbon fluxes measured with eddy covariance. Remote Sensing of Environment 133, 102-115.